arXiv:0711.1470v1 [nucl-ex] 9 Nov 2007

Source shape determination with directional fragment-fragment velocity correlations

A. Le Fèvre [a], C. Schwarz [a], G. Auger [b],
M.L. Begemann-Blaich [a], N. Bellaize [c], R. Bittiger [a],
F. Bocage [c], B. Borderie [d], R. Bougault [c], B. Bouriquet [b],
J.L. Charvet [e], A. Chbihi [b], R. Dayras [e], D. Durand [c],
J.D. Frankland [b], E. Galichet [d,k], D. Gourio [a], D. Guinet [f],
S. Hudan [b], P. Lautesse [f], F. Lavaud [d], R. Legrain [e,1], O. Lopez [c],
J. Łukasik [a,j], U. Lynen [a], W.F.J. Müller [a], L. Nalpas [e],
H. Orth [a], E. Plagnol [d], E. Rosato [g], A. Saija [h], C. Sfienti [a],
B. Tamain [c], W. Trautmann [a], A. Trzciński [i], K. Turzó [a],
E. Vient [c], M. Vigilante [g], C. Volant [e], B. Zwiegliński [i]

The INDRA and ALADIN Collaborations

[a] *Gesellschaft für Schwerionenforschung mbH, D-64291 Darmstadt, Germany*

[b] *GANIL, CEA et IN2P3-CNRS, F-14076 Caen, France*

[c] *LPC Caen, ENSICAEN, Université de Caen, CNRS/IN2P3, F-14050 Caen, France*

[d] *Institut de Physique Nucléaire, IN2P3-CNRS et Université, F-91406 Orsay, France*

[e] *DAPNIA/SPhN, CEA/Saclay, F-91191 Gif sur Yvette, France*

[f] *Institut de Physique Nucléaire, IN2P3-CNRS et Université, F-69622 Villeurbanne, France*

[g] *Dipartimento di Scienze Fisiche e Sezione INFN, Univ. Federico II, I-80126 Napoli, Italy*

[h] *Dipartimento di Fisica dell' Università and INFN, I-95129 Catania, Italy*

[i] *A. Sołtan Institute for Nuclear Studies, Pl-00681 Warsaw, Poland*

[j] *H. Niewodniczański Institute of Nuclear Physics, Pl-31342 Kraków, Poland*

[k] *Conservatoire National des Arts et Métiers, F75141 Paris cedex 03, France*

Abstract

Correlation functions, constructed from directional projections of the relative velocities of fragments, are used to determine the shape of the breakup volume in coordinate space. For central collisions of ^{129}Xe + $^{\mathrm{nat}}$Sn at 50 MeV per nucleon incident energy, measured with the 4π multi-detector INDRA at GSI, a prolate shape aligned along the beam direction with an axis ratio of 1:0.7 is deduced. The sensitivity of the method is discussed in comparison with conventional fragment-fragment velocity correlations.

Key words: Heavy ion collisions, multifragmentation, breakup state, correlation functions
PACS: 25.70.Pq, 24.60.-k, 25.75.Gz

A recent study of central ^{129}Xe+$^{\mathrm{nat}}$Sn and ^{197}Au+^{197}Au collisions at bombarding energies between 50 and 100 MeV per nucleon has shown that a good statistical description of the measured fragment yields and kinetic energies can be obtained provided that a prolate source deformation and a superimposed collective motion are included [1]. The experimental data had been collected with the 4π INDRA multidetector [2] at the GSI laboratory. The statistical model employed in this study was the Metropolis Multifragmentation Monte-Carlo (MMMC) model [3] which had been extended to non-spherical (NS) sources [4], a version referred to in the following as MMMC-NS model. The MMMC Statistical Model is based on the microcanonical ensemble and has found many applications in nuclear multifragmentation (see, e.g., [3,5,6,7,8]).

A prolate deformation of the emitting source along the direction of the incident beam was indicated by the observed anisotropies of the fragment production. The element spectra were found to extend to larger atomic numbers Z at forward and backward emission angles than at sideward angles. The largest fragment within an event is preferentially emitted toward forward or backward angles. If emitted sidewards, its mean Z decreases, e.g., from $Z \approx 18$ at $\theta_{\mathrm{cm}} = 0^\circ$ to $Z \approx 14$ at $\theta_{\mathrm{cm}} = 90^\circ$ for the 1% most central collisions of ^{129}Xe+$^{\mathrm{nat}}$Sn at 50 MeV per nucleon, selected on the basis of the measured charged-particle multiplicity or the transverse energy of light charged particles [1].

In the model description, an important role is played by the Coulomb interaction which favours large separations between heavy fragments in order to minimize the Coulomb energy. Heavy fragments are, therefore, preferentially placed in the tips of a prolate source. Coulomb repulsion and the superimposed radial flow transform these spatial correlations into correlations in momentum space which produces the observed maxima in the yields and kinetic energies of the heaviest fragments at forward and backward directions. The orientation along the beam axis is clearly of a dynamical origin. The question, therefore, arises whether the deformation of the model source, besides the superimposed flow, is mainly required for simulating the observed anisotropies in momentum space or whether it actually reflects the source shape at breakup as caused by the reaction dynamics.

---

[1] deceased
[2] corresponding author: w.trautmann@gsi.de

It is the aim of the present work to confirm the indicated source deformations in coordinate space by applying interferometric methods to the same data, here at first only for the case of ^{129}Xe+$^{\mathrm{nat}}$Sn at 50 MeV per nucleon. Interferometry has become a standard tool for investigating the space-time properties of the breakup state in heavy-ion reactions [9,10,11]. The spatial dimensions or space and time are usually separated by exploiting the effects of quantum statistics in proton-proton, neutron-neutron, or pion-pion correlation functions [10,12,13,14,15,16]. Particle pairs are selected according to the orientation of their relative velocity with respect to the chosen coordinate axes, and separate correlation functions are generated as, e.g., for longitudinal and transverse orientations. In fragmentation reactions, the mutual Coulomb repulsion between fragment pairs has been used to derive time scales for the emission process from fragment-fragment correlation functions [17,18,19,20,21]. Glasmacher et al. have shown that also information on the source geometry can be obtained if directional cuts are applied and correlation functions are generated for fragment pairs with relative velocities parallel or perpendicular to the symmetry axis [22,23]. The dependence on the source geometry was small, even though nuclei with the unusual shapes of flat disks or toroids were included in these studies. It will be shown in the following that the sensitivity to the source geometry is significantly enhanced with the proposed new kind of correlation functions of projections.

The new correlation functions are constructed from the relative velocities of fragment pairs by not using their modulus, as for conventional fragment-fragment correlations, but rather their longitudinal and transverse components with respect to the direction of orientation which here is the beam axis. To correct, in first order, for the variation of the Coulomb repulsion with the fragment Z, the reduced velocity $v_{\mathrm{red}} = v_{\mathrm{rel}}/\sqrt{Z_i + Z_j}$ is used, where v_{rel}, Z_i and Z_j are the relative velocity and the atomic numbers of the two fragments, respectively [24]. With the help of model calculations, it will be shown that these projected correlations are particularly sensitive to a deformation of the source. This will be done in comparison to conventional correlation functions generated not with directional cuts but with directional weights, proportional to $\sin^2\theta$ and $\cos^2\theta$ where θ is the polar angle of the relative velocity vector with respect to the beam axis [16]. The method will then be applied to the experimental data for the ^{129}Xe+$^{\mathrm{nat}}$Sn reaction at 50 MeV per nucleon.

Experimental details of these measurements, performed at the GSI laboratory in 1998 and 1999, and of the analysis and calibration procedures may be found in [1,25,26,27]. Natural Sn targets of areal density 1.05 mg/cm^2 were

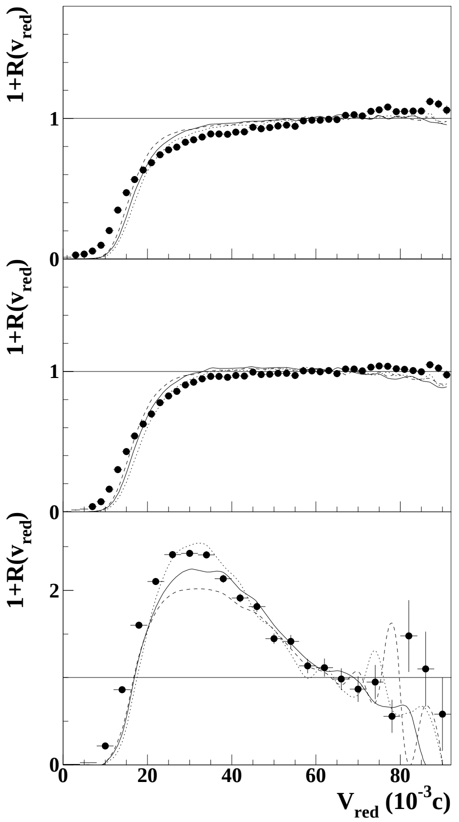

Fig. 1. Fragment-fragment velocity correlations as a function of the reduced velocity v_{red} (in units of $10^{-3}c$) of fragment pairs with $3 \leq Z \leq 30$ (top and middle panels) and of the two fragments with the largest Z within an event (bottom panel) for central collisions of ^{129}Xe+$^{\mathrm{nat}}$Sn at 50 MeV per nucleon (dots). Solid, dashed and dotted lines represent the filtered predictions of the MMMC-NS model for the prolate, oblate and spherical sources, respectively. The uncorrelated denominator was generated after azimuthal event alignment for the top panel and after polar event alignment for the middle and bottom panels (see text). The interval $50 - 100 \cdot 10^{-3}c$ is chosen for normalization.

bombarded with ^{129}Xe beams delivered by the SIS heavy-ion synchrotron. Central impact parameters were selected by requiring that the total transverse energy $E_{\perp 12}$ of light charged particles (Z = 1,2) exceeded 637 MeV [1]. This corresponds to an impact-parameter range $b/b_{\mathrm{max}} \leq 0.1$, according to the geometrical prescription of [28].

Standard fragment-fragment velocity correlations constructed for this event class are shown in Fig. 1. They were obtained with the technique of event mixing, and the interval $50 - 100 \cdot 10^{-3}c$ was chosen for normalization (c is the velocity of light). In the top panel, the uncorrelated denominator was generated after rotating all events, azimuthally with respect to the beam axis, into a common reaction plane in order to suppress artificial flow effects [29]. The orientation of an event was determined from that of the longest eigenvector of the kinetic-energy tensor, built from all detected charged particles. A flat correlation function at large v_{red} is obtained by aligning all events with respect to each other before generating the uncorrelated denominator, e.g. by rotating their longest eigenvectors into the beam direction (Fig. 1, middle panel). With this polar event alignment, the distribution of mixed pairs extends to slightly larger v_{red}, leading to a reduction of $1+R$ with respect to the case of azimuthal alignment only (top panel). The simpler method of azimuthal event alignment has, nevertheless, been used in the analysis described below (Figs. 2-4).

All correlation functions are characterized by a strong suppression of small relative velocities, with $1+R$ falling below 0.5 for $v_{\mathrm{red}} \leq 14 \cdot 10^{-3}c$. Similarly large suppressions have been observed for a variety of heavy-ion and light-ion induced reactions and were consistently interpreted as indicating short breakup times of the order of 50 - 100 fm/c [20,23,30,31]. The correlation function of the pairs with largest Z in each event (Fig. 1, bottom panel) exhibits a considerable enhancement around $30 \cdot 10^{-3}c$. With mean values $\langle Z_1 \rangle = 13$ for the largest and $\langle Z_2 \rangle = 8$ for the second largest fragment [1], the bump corresponds to relative velocities of ≈ 4 cm/ns, a value typically observed for large-angle fragment-fragment correlations [6,32]. The distribution of relative angles between the two largest fragments in the center-of-mass system is indeed wide and has a mean value of $\approx 100°$.

The MMMC-NS model [4] has been used as an event generator for constructing correlation functions to be compared with the experimental data. For the global source parameters the previously obtained values of total charge $Z = 79$ and mass $A = 188$, excitation energy $E_x = 6$ MeV per nucleon, and collective flow 2 MeV per nucleon with a profile parameter $\alpha_{\mathrm{coll}} = 2$ were used [1]. Only the shape parameters were varied, and three different source elongations were chosen, a prolate source with axis ratio 1:0.70, an oblate source with axis ratio 1:1.67, and a spherical source. The produced MMMC-NS events have been filtered using a software replica of the experimental apparatus that takes into account the main properties of the INDRA multidetector as, e.g., the exact geometry of the detectors, the energy thresholds and limits for charged-particle detection and identification, and the effects of the multihit treatment in the off-line analysis.

The standard correlation functions depend very weakly on the source shape (Fig. 1). Only the correlation function for the two largest fragments exhibits slightly different maxima for deformed sources whose normalization, however, in the absence of an uncorrelated plateau region, is less certain (Fig. 1, bottom panel). The depression at small v_{red} is well reproduced, even though the predicted rise around $v_{\mathrm{red}} = 15 \cdot 10^{-3}c$ is steeper than found experimentally. Smoother correlation functions could probably be generated and a better agreement reached with finite emission times and by allowing the source parameters to fluctuate (cf. Ref. [33]).

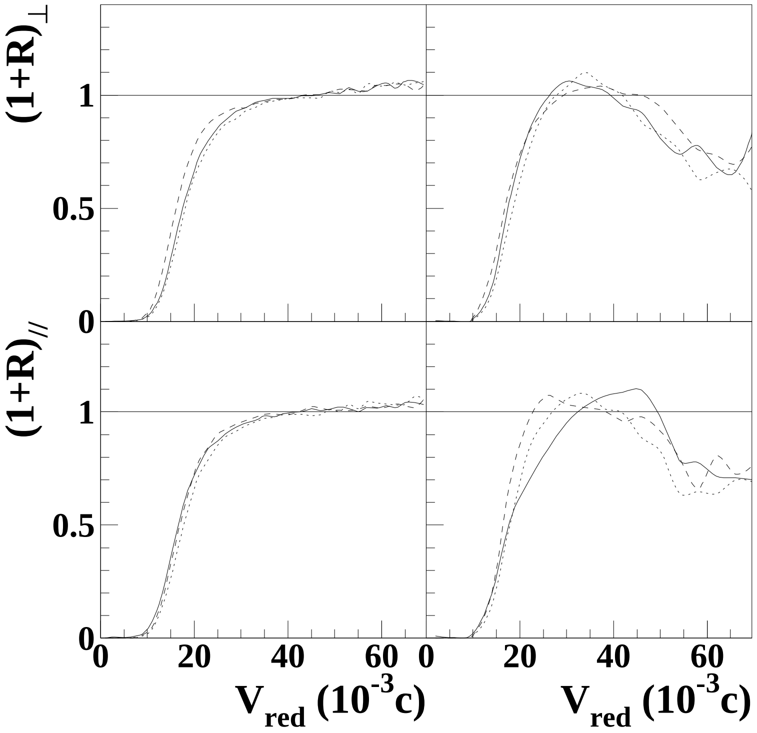

Fig. 2. Directional correlation functions obtained from filtered predictions of the MMMC-NS model for fragment pairs with $3 \leq Z \leq 30$ (left panels) and for the two fragments with largest Z within each event (right panels). The top and bottom panels show the transverse and longitudinal correlation functions, respectively, obtained with the method of directional weights [16]. Solid, dashed and dotted lines represent the predictions for the prolate, oblate and spherical sources, respectively. The interval $30 - 100 \cdot 10^{-3}c$ is chosen for normalization.

The dependence of conventional directional fragment-fragment correlation functions on the shape of the emitting source in coordinate space is illustrated in Fig. 2. Longitudinal and transverse correlation functions were generated with the method of directional weights [16], i.e. by accumulating the numerators and denominators with weight functions $\cos^2\theta$ and $\sin^2\theta$, respectively. Their dependence on the source shape is visible but weak, similar to the results reported in [22,23].

A much stronger sensitivity to the deformation is exhibited by the correlation functions generated separately for the longitudinal and transverse projections of the relative velocity v_{red} (Fig. 3). Note that for the projections shown here and below different intervals were chosen for normalization (see captions). Since individual components can become small even if the modulus of v_{red} is large, these correlation functions do not approach zero at small values of the projected v_{red}. Their magnitude there is sensitive to correlations of the orientations of the relative-velocity vectors which, apparently, depend strongly on the source shape. The correlations of the transverse projections at small

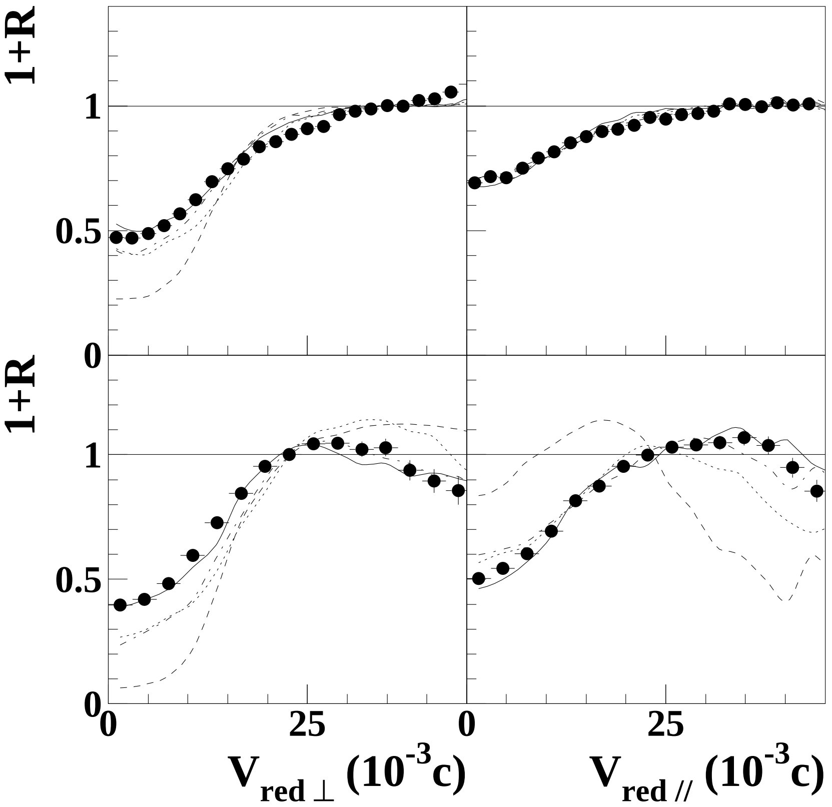

Fig. 3. Correlation functions constructed from the transverse (left panels) and longitudinal (right panels) projections of the reduced relative velocity of fragment pairs with $3 \leq Z \leq 30$ (top panels) and of the two fragments with largest Z (bottom panels) for central ^{129}Xe+$^{\mathrm{nat}}$Sn collisions at 50 MeV per nucleon (symbols). Solid, dashed and dotted lines represent the filtered predictions of the MMMC-NS model for the prolate, oblate and spherical sources, respectively. The dashed-dotted lines (closely following the dotted lines at small v_{red}) represent the spherical source with ellipsoidal flow (see Ref. [1]). The normalization was performed, individually for each projection, within $30 - 40 \cdot 10^{-3}c$ in the top and $20 - 30 \cdot 10^{-3}c$ in the bottom panels, respectively.

$v_{\mathrm{red}\perp}$, in particular, change significantly with the source geometry. As will be shown and discussed below, the sensitivity to radial flow is large as well. With the flow value 2 MeV per nucleon determined from the fragment kinetic energies, a good agreement with the experimental data for ^{129}Xe+$^{\mathrm{nat}}$Sn is reached by assuming a prolate deformation. This is valid for the correlation functions generated from all pairs with $Z_{i,j} > 2$ but, in particular, also for the correlation functions for the two largest fragments of each partition (Fig. 3, bottom). The comparison thus confirms the conclusions drawn from the study of the fragment anisotropies in yields and kinetic energies [1].

Projected correlation functions generated with the MMMC model for central ^{129}Xe+$^{\mathrm{nat}}$Sn collisions with the same input parameters but with the collective

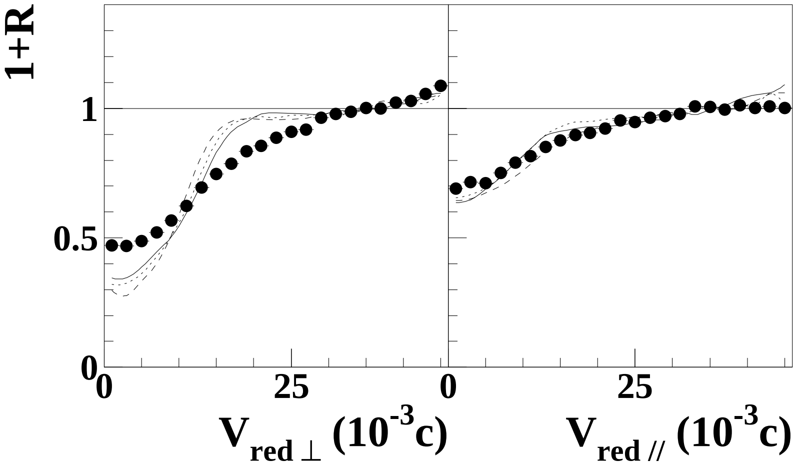

Fig. 4. Correlation functions constructed from the transverse (left panel) and longitudinal (right panel) projections of the reduced relative velocity of fragment pairs with $3 \leq Z \leq 30$ for central ^{129}Xe+$^{\rm nat}$Sn collisions at 50 MeV per nucleon (symbols, same data as in Fig. 3, top panels). Solid, dashed and dotted lines represent the predictions of the MMMC-NS model without radial flow for the prolate, oblate and spherical sources, respectively. The normalizations were performed within $30 - 40 \cdot 10^{-3}c$.

radial flow set to zero are shown in Fig. 4. Without flow, their rise at small $v_{\rm red}$ is much steeper, notably for the transverse projections, and their differences for the three considered source shapes are much smaller. It is evident that the experimental data for ^{129}Xe+$^{\rm nat}$Sn are qualitatively different from this set of correlation functions and cannot be reproduced without assuming collective contributions to the particle and fragment energies.

The deduced sensitivities to the source shape in coordinate space were independently verified by reproducing the experimental correlation functions with a simpler source model [34]. Fragments were sampled according to the experimental yield distribution and placed randomly without overlap into a predetermined ellipsoidal volume with the transverse (R_x, R_y) and longitudinal (R_z) source radii being varied between 6 fm and 30 fm. The parameters describing the thermal and anisotropic collective motions of the fragments were chosen, individually as a function of Z, so as to best reproduce the measured kinetic energies. The temporal evolution after freeze-out was modeled with N-body Coulomb trajectory calculations. The asymptotic velocities were used to construct both, weighted and projected, correlation functions. The result of a comparison with the experimental data, for intermediate-mass fragments with $5 \leq Z \leq 7$, is shown in Fig. 5 in the form of the χ^2 distributions in the plane of the transverse and longitudinal extensions, representing the degree of agreement obtained.

The different sensitivities of the two types of correlation functions are imme-

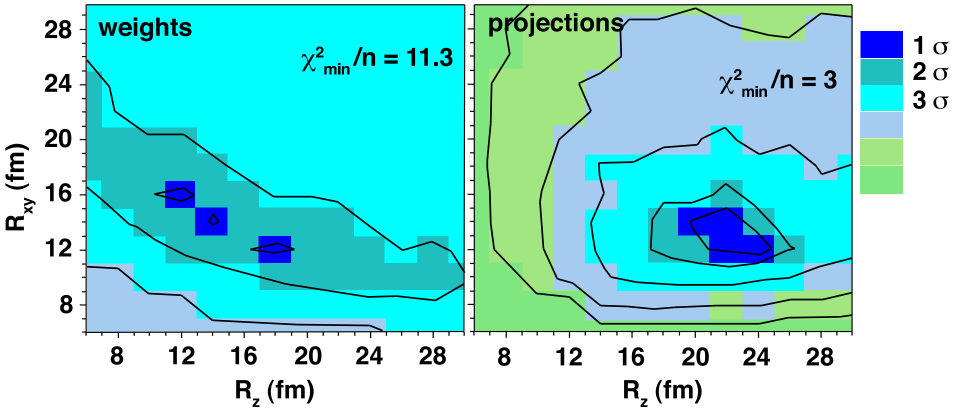

Fig. 5. (color online) Contour plots (in units of the standard deviation σ) of the two-dimensional χ^2 distributions in the plane of the transverse (xy) and longitudinal (z) extensions of the source, as obtained from the comparison of the experimental weighted (left panel) and projected (right panel) correlation functions, for fragments with $Z = 5-7$, with the predictions of the classical deformed-source model for ^{129}Xe+$^{\mathrm{nat}}$Sn at 50 MeV per nucleon.

diately apparent. With directional weights, the minima of the χ^2 distribution extend over a broad band of radius values, all corresponding to approximately the same volume but to different shapes. For the correlation functions constructed from the projections (right panel of Fig. 5), the minima are concentrated in a region of prolate source shapes with axis ratios of $1 : 0.6 \pm 0.1$. Other observations were also found to be similar to those made with the more complex MMMC model. In particular, the requirement of a finite radial flow for obtaining the shape dependence of the projected correlation functions was confirmed. Radial flow leads to a correlation between the locations of a particle in coordinate space and in momentum space which makes its role here understandable. However, flow by itself is not sufficient (cf. dotted and dashed-dotted lines in Fig. 3). The projected correlation functions become significantly different only in the presence of deformations in coordinate space (full and dashed-dotted lines in Fig. 3).

The volumes obtained with this method are large. A mean radius of 15 fm (Fig. 5, left panel) corresponds to about twice the radius of a system of $A = 188$ nucleons at normal density, slightly larger than what is usually assumed in applications of the MMMC model (6 times the normal nuclear volume in Refs. [1]) or what is obtained with other methods [35,36]. A very similar volume results from the transverse and longitudinal radii of 13 fm and 22 fm, respectively, favoured by the method of projections (Fig. 5, right panel). Considering the finite range of Z used for this comparison, this is perhaps not unreasonable. It is, furthermore, known that large variations of the volume are necessary in order to change fragment-fragment correlation functions significantly [37]. An additional contribution to the apparent source size may also come from the finite time scale of the emission process even though it is expected to be rather short, perhaps 50 - 100 fm/c (see, e.g., Ref. [23,38]). Estimates for the increase of the mean source radius, obtained from simulations with the above-mentioned simpler source model using finite emission times, are of the order of 1 - 2 fm. They are non-negligible regarding the corresponding breakup volume but they are unlikely to change the parameters describing its anisotropy.

In summary, a new method based on correlation functions of relative-velocity projections has been presented and shown to be sensitive to source deformations in the presence of flow. It has been applied to the data for central collisions of ^{129}Xe+$^{\rm nat}$Sn at 50 MeV per nucleon, and an expanded source with a prolate elongation in the direction of the incident beam has been deduced. The axis ratio 1 : 0.7 used for the quantitative comparison with the MMMC-NS model predictions has led to very satisfactory results, thus supporting the assumption of a non-spherical breakup source with a deformation of this magnitude for the statistical description of the fragmentation channels with this model [1]. A similar deformation of $1 : 0.6 \pm 0.1$ has resulted from the analysis with a simpler source model, restricted to the Z = 5-7 range of fragments.

The dynamical origin of this deformation was not a subject of the present study but is most likely found in the incomplete mutual stopping of the incident ions, even in the most violent collisions associated with the largest transverse energies or particle multiplicities. Stopping is incomplete even in the heavier ^{197}Au+^{197}Au system for which an excitation function of stopping with a maximum at several hundred MeV per nucleon has been established [39,40]. At the present energy of 50 MeV per nucleon and below, the observed mass hierarchy of the longitudinal fragment velocities provides further evidence for dynamical correlations between the entrance and exit channels [41]. In coordinate space, the larger longitudinal momenta will cause the source shape to be elongated at the time when the breakup density has been reached. Larger fragments, presumably carrying most of the remaining longitudinal momentum, will be near the tips of the elongated source, an effect which in the static MMMC-NS description is generated by the Coulomb force alone. Coulomb effects are probably less dominant in the dynamical situation which explains why the deformed-source model, by its construction, permits exploring the statistical nature of multi-fragment breakups in the presence of dynamical constraints which are not part of the model. Source deformations and anisotropic emissions are generic features of central collisions at intermediate energies, a fact already quite well established but supported in a new way with the present method. Since the radial flow is increasing it should be possible to extend these studies to higher bombarding energies.

This work was supported by the European Community under contract No. ERBFMGECT950083.

References

[1] A. Le Fèvre et al., Nucl. Phys. A **735** (2004) 219.

[2] J. Pouthas *et al.*, Nucl. Inst. and Meth. in Phys. Res. A **357** (1995) 418.

[3] D.H.E. Gross, Rep. Prog. Phys. **53** (1990) 605.

[4] A. Le Fèvre, M. Płoszajczak, V.D. Toneev, Phys. Rev. C**60** (1999) 051602.

[5] D.H.E. Gross, K. Sneppen, Nucl. Phys. A **567** (1994) 317.

[6] Bao-An Li, D.H.E. Gross, V. Lips, H. Oeschler, Phys. Lett. B **335** (1994) 1.

[7] M. Begemann-Blaich *et al.*, Phys. Rev. C **58** (1998) 1639.

[8] A.S. Botvina and I.N. Mishustin, Eur. Phys. J. A **30** (2006) 121.

[9] D. Ardouin, Int. J. Mod. Phys. **E6** (1997) 391.

[10] U.A. Wiedemann, U. Heinz, Phys. Rep. **319** (1999) 145.

[11] G. Verde *et al.*, Eur. Phys. J. A **30** (2006) 81.

[12] S.E. Koonin, Phys. Lett. B **70** (1977) 43.

[13] M.A. Lisa *et al.*, Phys. Rev. Lett. **71** (1993) 2863.

[14] N. Colonna *et al.*, Phys. Rev. Lett. **75** (1995) 4190.

[15] U. Heinz, B.V. Jacak, Annu. Rev. Nucl. Part. Sci **49** (1999) 529.

[16] C. Schwarz *et al.*, Nucl. Phys. A **681** (2001) 279c.

[17] R. Trockel *et al.*, Phys. Rev. Lett. **59** (1987) 2844.

[18] D. Fox *et al.*, Phys. Rev. C **50** (1994) 2424.

[19] L. Beaulieu *et al.*, Phys. Rev. Lett. **84** (2000) 5971.

[20] V.K. Rodionov *et al.*, Nucl. Phys. A **700** (2002) 457.

[21] G. Tăbăcaru *et al.*, Nucl. Phys. A **764** (2006) 371.

[22] T. Glasmacher, C.K. Gelbke, S. Pratt, Phys. Lett. B **314** (1993) 265.

[23] T. Glasmacher *et al.*, Phys. Rev. C **50** (1994) 952.

[24] Y.D. Kim *et al.*, Phys. Rev. C **45** (1992) 338.

[25] J. Łukasik *et al.*, Phys. Rev. C **66** (2002) 064606.

[26] A. Trzciński *et al.*, Nucl. Inst. and Meth. in Phys. Res. A **501** (2003) 367.

[27] K. Turzó *et al.*, Eur. Phys. J. A **21** (2004) 293.

[28] C. Cavata *et al.*, Phys. Rev. C **42** (1990) 1760.

[29] R. Kotte *et al.*, Phys. Rev. C **51** (1995) 2686.

[30] O. Lopez *et al.*, Phys. Lett. B **315** (1993) 34.

[31] G. Wang *et al.*, Phys. Rev. C **60** (1999) 014603.

[32] J. Pochodzalla, W. Trautmann, U. Lynen, Phys. Lett. B **232** (1989) 41.

[33] Y.D. Kim *et al.*, Phys. Rev. C **45** (1992) 387.

[34] A. Le Fèvre et al., in: I. Iori, A. Moroni (Eds.), Proceedings of the XLIst International Winter Meeting on Nuclear Physics, Bormio, Italy, 2003, Ricerca Scientifica ed Educazione Permanente Suppl., vol. 120, Milano, 2003, p. 178.

[35] M. Pârlog *et al.*, Eur. Phys. J. A **25** (2005) 223.

[36] S. Piantelli *et al.*, Phys. Lett. B **627** (2005) 18.

[37] O. Schapiro, A.R. DeAngelis, D.H.E. Gross, Nucl. Phys. A **568** (1994) 333.

[38] K. Zbiri *et al.*, Phys. Rev. C **75** (2007) 034612.

[39] W. Reisdorf *et al.*, Phys. Rev. Lett. **92** (2004) 232301.

[40] A. Andronic *et al.*, Eur. Phys. J. A **30** (2006) 31.

[41] J. Colin *et al.*, Phys. Rev. C **67** (2003) 064603.